Biophysical Journal Volume 98 April 2010 1209–1217

Deuterium NMR Study of the Effect of Ergosterol on POPE Membranes

Ya-Wei Hsueh,[†‡§*] Chi-Jung Weng,[†] Mei-Ting Chen,[†] Jenifer Thewalt,[¶‖] and Martin Zuckermann[¶]
[†]Department of Physics, [‡]Center for Complex Systems, and [§]Institute of Biophysics, National Central University, Jhong-li 320, Taiwan; and
[¶]Department of Physics and [‖]Department of Molecular Biology and Biochemistry, Simon Fraser University, Burnaby, British Columbia, Canada

ABSTRACT We study the effect of ergosterol on the physical properties of 1-[$^2H_{31}$]palmitoyl-2-oleoyl-*sn*-glycero-3-phosphoethanolamine (POPE) multibilayers using deuterium nuclear magnetic resonance. NMR spectra were taken as a function of temperature and ergosterol concentration up to 70 mol %. The spectral first moments show that there is a dramatic difference in the ability of ergosterol to disorder the gel phase and to order the liquid-crystalline phase of POPE membranes, an unusual behavior among lipid/sterol systems studied up to now. Further investigation of the liquid-crystalline phase shows that ergosterol (erg) increases the chain order of POPE-d31, but that this effect saturates at 10 mol % ergosterol. This is in marked contrast to the effect of cholesterol (chol) on POPE membranes: the chain order of POPE increases with cholesterol to at least 45 mol %. Moreover, we found that at higher ergosterol concentrations (>40 mol %) ergosterol decreases the POPE-d31 chain order, which, to our knowledge, has not been directly observed in other lipid/sterol systems. The temperature-composition phase diagram is presented. Finally, at all ergosterol concentrations, the chain order of liquid-crystalline-phase POPE is much smaller than that of comparable POPE/chol membranes. This implies that there is no liquid-ordered phase behavior for POPE/erg membranes.

INTRODUCTION

Sterols are essential components of the plasma membranes (PMs) of eukaryotic cells. In particular, cholesterol is ubiquitous in the PMs of mammalian cells (1) and ergosterol is the major sterol in certain fungi and protozoans (2,3). These sterols play fundamental roles in biological membrane structure and function. Like cholesterol in mammalian cell PMs, ergosterol in yeast cell PMs is implicated to be associated with lipid rafts (4) that affect the function of yeast membrane proteins (5–7). The domain structure of yeast PMs can also modulate interactions with mammalian proteins. For example, a protein involved in Parkinson's disease, α-synuclein, was shown recently to associate with yeast PM rafts in an ergosterol-dependent manner (7). Knowledge of the physical properties of biological membranes is needed to interpret such observations. To gain a better understanding of the effect of sterols on biological membrane properties requires investigations of the phase behavior of lipid/sterol systems.

Studies of two-component phosphatidylcholine (PC)/sterol membranes have shown the formation of a liquid-ordered phase at high sterol concentrations (8–12). Coexistence of liquid-disordered and liquid-ordered (lo) phases were observed in some PC/sterol mixtures at intermediate sterol concentration using various techniques (8,9,11–13). In addition, the effects of sterols on PC membrane organization are opposite below and above the main transition of lipid. Sterols tend to loosen lipid packing in the gel phase, while increasing hydrophobic chain order leading to tighter lipid packing in the liquid-crystalline phase (11,13,14). Comparative studies of different sterols on PC membranes were also carried out (15–18) and showed that slight structural alterations of sterols can markedly affect the membrane properties. Much attention has been focused on PC/sterol systems, whereas phosphatidylethanolamine (PE)/sterol membrane organization remains less explored. PE/sterol lipid interactions are of great interest as PE is the second most abundant phospholipid class in the PMs of yeast *Saccharomyces cerevisiae* (19) and mammalian cells. PE furthermore is the primary phospholipid component of the cytoplasmic leaflet of mammalian PMs.

The phase behavior of pure 1-[$^2H_{31}$]palmitoyl-2-oleoyl-*sn*-glycero-3-phosphoethanolamine (POPE) membranes is as follows: a main transition between gel and lamellar liquid-crystalline (lc) phases at 25°C, and a transition between lc and inverted hexagonal (H_{II}) phases at 71°C. Paré and Lafleur studied POPE/chol membranes by deuterium nuclear magnetic resonance (^{2}H NMR) and Fourier transform infrared spectroscopy (20). They found that cholesterol induces the formation of a lo phase as observed previously for PC/chol membranes. In particular the temperature-composition phase diagram of POPE/chol exhibits a gel-lo phase coexistence region as was also observed for DPPE/chol (21). Cholesterol loosens PE chain packing in the gel phase and increases PE chain order in the lc phase (20–22), as in the case of PC/chol membranes.

^{2}H NMR is a noninvasive method for the investigation of the physical properties of model membranes and has been used widely to study the order parameter of lipid-sterol membranes from measurements of the first spectral moment, M_1. For example, it was found that the average chain order of POPE increases with increasing cholesterol concentration up to at least 45 mol % (20). Similar results were observed in various PC/sterol systems in the sterol concentration range mostly below 50 mol % (13,14). Saturation of membrane properties has been reported for other PC/sterol systems.

Submitted August 6, 2009, and accepted for publication December 3, 2009.
*Correspondence: yhsueh@cc.ncu.edu.tw
Editor: Peter Tieleman.

0006-3495/10/04/1209/9 $2.00
doi: 10.1016/j.bpj.2009.12.4279

For example M_1 saturates for POPC/erg membranes at 25 mol % ergosterol at 25°C, that was interpreted in terms of ergosterol solubility (13). Furthermore, x-ray examination of various POPC/sterol systems shows that the bilayer thickens with increasing sterol up to 20 mol %, then ceases to thicken further (23).

In this work, we studied the physical properties and phase behavior of POPE/erg membranes by ^{2}H NMR. The *sn*-1 chain of POPE was perdeuterated. The phase behavior of POPE/erg membranes was studied as a function of temperature and composition to a maximum concentration of 70 mol % ergosterol. POPE/chol membranes of several compositions were also studied by ^{2}H NMR for comparison. Using the information provided by ^{2}H NMR, we present a comprehensive examination of the effect of ergosterol on membrane phase state and acyl chain order. Our discussion will focus chiefly on lamellar phases. The temperature-composition phase diagram of POPE/erg is proposed. In addition, POPE/erg and POPE/chol membranes will be compared, and differences between the effects of ergosterol and cholesterol on membrane properties will be addressed.

MATERIALS AND METHODS

POPE-d31 was obtained from Avanti Polar Lipids (Alabaster, AL). Ergosterol (97% pure) was obtained from Fluka (Buchs, Switzerland). Cholesterol (99% pure) and deuterium-depleted water were obtained from Sigma-Aldrich (St. Louis, MO).

POPE-d31/erg multilamellar dispersions were prepared for ergosterol concentrations of 0, 2, 10, 20, 30, 40, 50, 65, and 70 mol %. POPE-d31/chol multilamellar dispersions were prepared for cholesterol concentrations of 20 and 30 mol %. POPE-d31 and sterol were mixed in the appropriate quantities, dissolved in benzene/methanol, 4:1 (v/v) and then freeze-dried. Samples were hydrated using a pH 7.4 buffer prepared in deuterium-depleted water containing 50 mM HEPES, 150 mM NaCl, 4 mM EDTA. Hydration was carried out by freeze-thaw-vortex cycling five times between liquid nitrogen temperature and 45–50°C.

^{2}H NMR experiments were carried out on Varian NMR spectrometer (Infinity plus 300) at 46.06 MHz using the quadrupolar echo technique (24). The typical spectrum resulted from 10,000−20,000 repetitions of the two-pulse sequence with 90° pulse lengths of 3.95 μs, interpulse spacing of 40 μs and dwell time 2 μs. The delay between acquisitions was 300 ms and data were collected in quadrature with Cyclops 8-cycle phase cycling. The spectra were dePaked using the procedure described by Lafleur et al. (25). All POPE-d31/erg spectra were acquired from 5°C to 69°C, except 30:70 POPE-d31/erg that was measured only at 25°C. POPE-d31/chol spectra were acquired from 5°C to 43°C. At each temperature, the sample was allowed to equilibrate for 20–30 min before a measurement. The first moment, M_1, was calculated from the spectrum using

$$M_1 = \frac{1}{A}\sum_{\omega=-x}^{x} |\omega| f(\omega), \qquad (1)$$

where ω is the frequency shift from the central (Larmor) frequency, $f(\omega)$ is the spectral intensity and $A = \sum_{\omega=-x}^{x} f(\omega)$.

M_1 is proportional to the average chain order parameter in the lc phase. The boundaries of a two-phase coexistence region can be determined by the spectral subtraction method (8,10,26). Within the two-phase region, each observed spectrum is simply a linear combination of the characteristic spectra for the two phases at the phase boundaries. The relative amount of gel and lc components is determined by the sample composition. Given two area-normalized observed spectra from samples of different composition at the same temperature, the characteristic spectra for the two phases at the phase boundary can be obtained by subtracting a fraction of one spectrum from the other. The phase boundaries then can be calculated using the lever rule. The spectral subtraction method is valid as long as certain assumptions hold. The exchange of labeled lipid between two kinds of domains must be slow on the NMR timescale so that it can be neglected. In addition, the domain must be sufficiently large, so that the signal from the lipid on the boundary of the domains is negligible.

The C–D bond order parameter, S_{CD}, is related to the quadrupolar splitting $\Delta\nu$ from a dePaked spectrum according to $\Delta\nu = 3/2(e^2qQ/h)S_{CD}$, where $(e^2qQ/h) = 167$ kHz is the static quadrupolar coupling constant (27). The smoothed order parameter profiles were determined from the dePaked spectra using a procedure described by Lafleur et al. (25). This approach assumes monotonic decrease of the order along the acyl chain and therefore reproduces only the smoothed features of the order variation.

RESULTS AND DISCUSSION

POPE-d31/ergosterol membranes

Fig. 1 shows the ^{2}H-NMR spectra of POPE-d31/erg as a function of ergosterol concentration at 18°C. Pure POPE-d31 has a gel phase spectrum at this temperature. The extra peaks near ±2.5 kHz and ±20 kHz in 2 and 10 mol % samples signal the emergence of an lc component. Furthermore, the proportion of lc component increases with increasing ergosterol concentration whereas the proportion of gel component decreases. This indicates that ergosterol

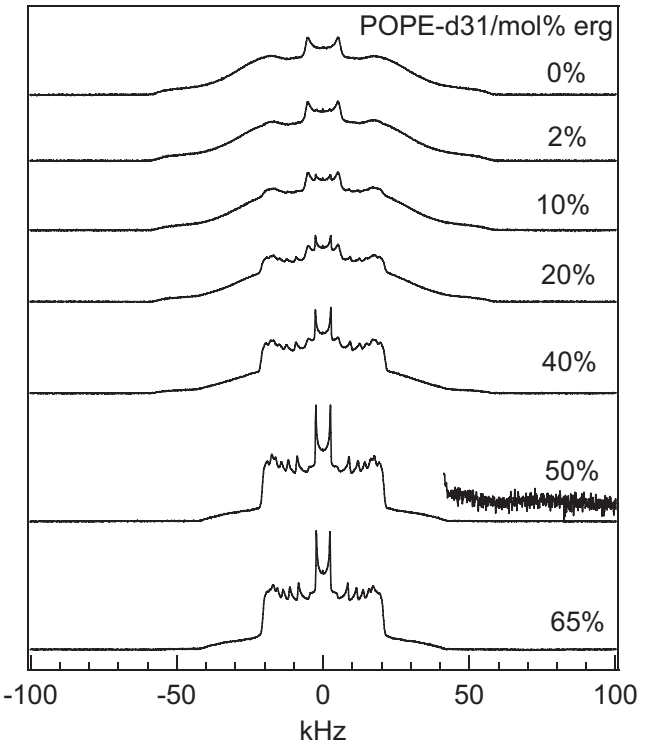

FIGURE 1 ^{2}H NMR spectra of POPE-d31/erg as a function of ergosterol concentration at $T = 18$°C.

promotes the formation of lc domains in gel-phase POPE-d31 membranes. The gel and lc phases coexist in samples containing 2−50 mol % ergosterol. At 65 mol % ergosterol, the POPE-d31 membranes are entirely in the lc phase, where the acyl chains undergo rapid, axially symmetric reorientation about the bilayer normal.

Spectral subtraction was used to separate the gel and lc components (the end-point spectra) from two spectra of different composition in the gel-lc phase coexistence region, and the ergosterol concentrations at phase boundaries (end-point concentrations) can be then determined. Fig. 2, *A* and *B*, show the gel and lc components, respectively, obtained from the measured spectra for 80:20 and 50:50 POPE-d31/erg at 15°C. The gel and lc end-point concentrations were calculated to be 12 and 62 mol % ergosterol, respectively. The spectra measured near these end-point concentrations are shown in Fig. 2, *C* and *D*, and are consistent with Fig. 2, *A* and *B*, respectively. This shows that the calculation of end-point concentrations is valid. Spectral subtractions were also carried out on measured spectra for 80:20 and 70:30 POPE-d31/erg, as well as those for 70:30 and 50:50 POPE-d31/erg. The gel and lc components are similar to those shown in Fig. 2, *A* and *B*, respectively. Moreover, the end-point concentrations calculated from these three sets of data agree within error. The above findings show that 80:20, 70:30, or 50:50 POPE-d31/erg samples are composed of gel and lc components at 15°C, confirming the coexistence of gel and lc phases inferred in Fig. 1. It is noted that the value of M_1 of Fig. 2 *B* (79,800 s^{-1}) is larger than that found for the lc phase of pure POPE ($M_1 = 6{,}6600\ s^{-1}$ at 23°C), but smaller than for the lo phase of POPE/chol ($M_1 = 91{,}500\ s^{-1}$ for 70:30 POPE-d31/chol at 17°C).

Fig. 3 gives the spectra of POPE-d31/erg as a function of ergosterol concentration at 29°C. For this temperature, pure POPE-d31 has an lc phase spectrum and Fig. 3 shows that addition of ergosterol does not affect this spectrum significantly. This is in contrast to the considerable change in the gel-phase spectra of Fig. 1 due to increasing ergosterol concentration. Furthermore, all POPE-d31/erg samples display sharp and well resolved individual peaks in the spectrum (see Fig. 3). Broadening of the individual peaks, which signals liquid-liquid phase coexistence (8,11,13), is not observed in this system. The properties of the lc phase will be discussed in detail later in this article.

Fig. 4 is a key figure as it gives $M_1(T)$ for POPE-d31/erg membranes for the whole range of both temperature and ergosterol concentration used in this work. We therefore discuss this data in detail. Two phase transitions are observed in $M_1(T)$ for pure POPE-d31 in Fig. 4. First, $M_1(T)$ for pure POPE-d31 (*open diamonds*) decreases abruptly near 22°C where the main transition, T_m, from the gel to the lc phase occurs. Furthermore, the rapid decrease in $M_1(T)$ at

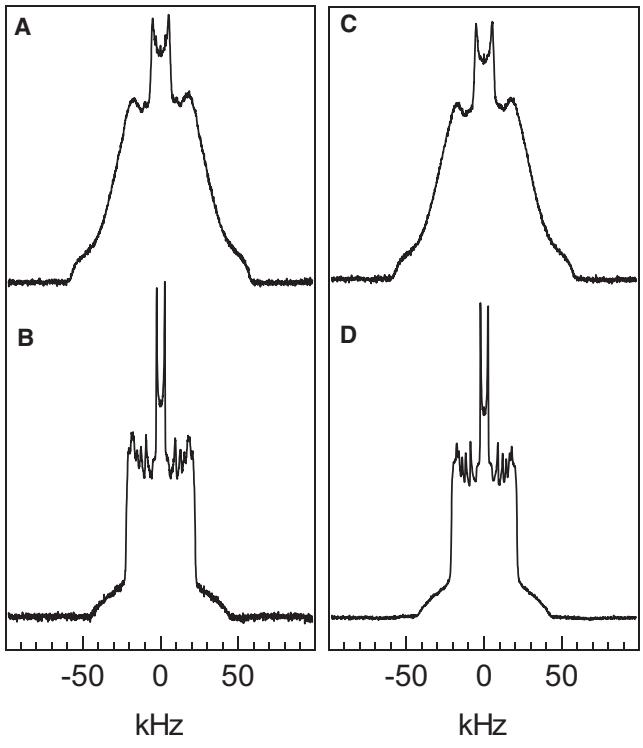

FIGURE 2 (*A* and *B*) Subtracted spectra obtained from the spectral subtraction of 80:20 and 50:50 POPE-d31/erg membranes at $T = 15°C$; ^2H NMR spectra of (*C*) 90:10 POPE-d31/erg at $T = 15°C$; and (*D*) 35:65 POPE-d31/erg at $T = 16°C$.

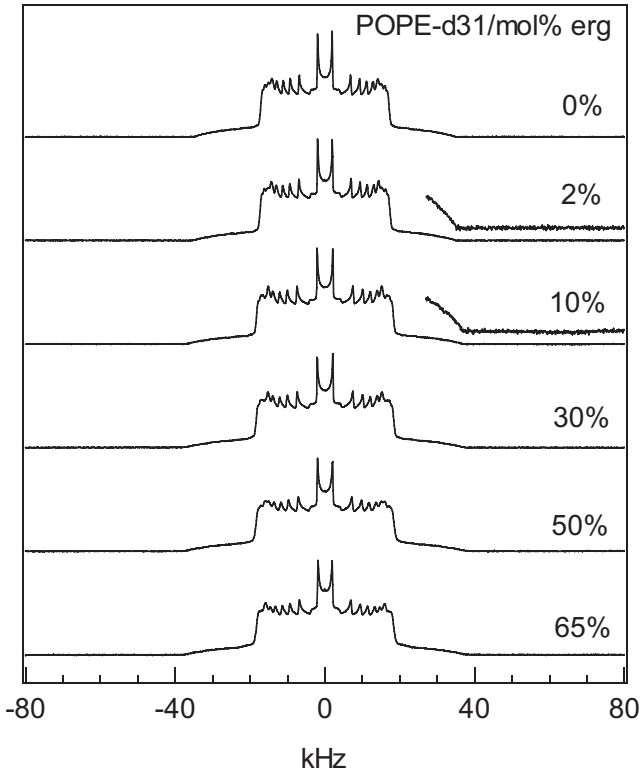

FIGURE 3 ^2H NMR spectra of POPE-d31/erg as a function of ergosterol concentration at $T = 29°C$.

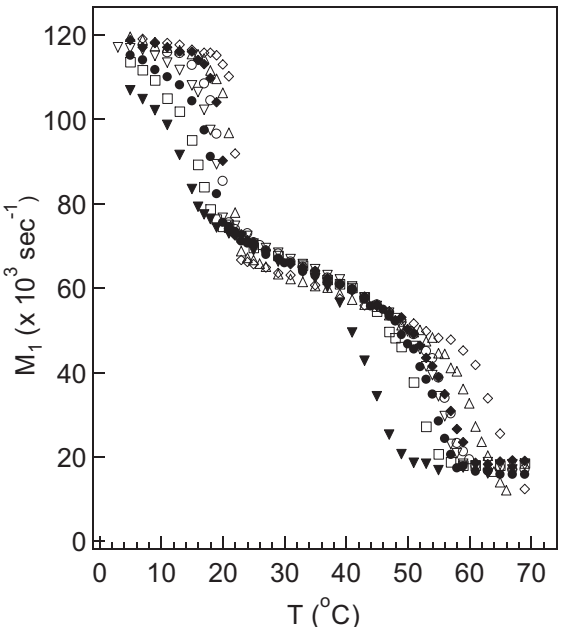

FIGURE 4 Temperature dependence of M_1 for POPE-d31/erg at various ergosterol concentrations. (◇) 0 mol %; (△) 2 mol %; (◆) 10 mol %; (○) 20 mol %; (▽) 30 mol %; (●) 40 mol %; (□) 50 mol %; and (▼) 65 mol %.

temperatures below T_m that is observed at all ergosterol concentrations can be attributed to the gel (or gel+ lc) to lc phase transition. A second rapid decrease in $M_1(T)$ at temperatures above 35°C can be ascribed to the lc to H_{II} phase transition. This will be discussed in the analysis of Fig. 7.

Fig. 4 shows that the value of M_1 for POPE-d31/erg decreases with increasing ergosterol concentration at temperatures below the completion of the main phase transition. This reflects the increasing proportion of lc phase in the membrane as ergosterol is added to POPE at these temperatures. Therefore addition of ergosterol disrupts the gel-phase POPE membrane. Similar effects were found for other lipid/sterol systems such as POPE/chol (20), DPPC/chol (8), and DPPC/erg (11). Fig. 4 also shows that M_1 for POPE/erg has only a weak dependence on ergosterol concentration between 22°C and ~35°C, where the membranes are in the lc phase. This is in contrast to the relatively strong ergosterol dependence in the gel or (gel + lc) regions of the phase diagram. Increasing the ergosterol concentration from 0 to 10 mol % increases M_1 by ~7% at 25°C. Because M_1 is proportional to the average chain order parameter in the lc phase, this shows that ergosterol increases the acyl chain order of POPE in this concentration range. However, no further ordering is observed as the ergosterol concentration is increased from 10 to 65 mol %: Fig. 4 shows that all $M_1(T)$ curves in this concentration range are quite close to each other. Thus the ability of ergosterol to order the acyl chains of POPE in the lc phase is quite limited.

Lipid/sterol systems such as DPPC/chol (8), DPPC/erg (11), and POPE/chol (see Fig. 9), exhibit similar features in terms of the effect of sterol: i), For all these systems, M_1 decreases with increasing sterol concentration in the gel or (gel + lc) regions of the phase diagram and increases with sterol concentration in the lc phase; and ii), when the sterol concentration increases, the decrease in M_1 of the gel-phase membrane and the increase in M_1 of the lc phase membrane are positively correlated. Fig. 4 shows that such a correlation is not observed in POPE/erg because M_1 decreases with increasing ergosterol concentration up to 65 mol % in the gel phase, whereas it increases with increasing ergosterol concentration only up to 10 mol % in the lc phase. There is thus a dramatic difference in the ability of ergosterol to disrupt the gel-phase and to order the lc-phase POPE membranes.

Fig. 5 shows M_1 for POPE-d31/erg as a function of ergosterol concentration in the lc phase at 25°C. M_1 first increases with ergosterol, saturates at 10 mol % ergosterol, and then decreases with increasing ergosterol above 40 mol %. This behavior has not as yet been observed in ^{2}H-NMR data for the lc phase of any other lipid/sterol system. In DPPC/chol (8), DPPC/erg (11), several POPC/sterol systems (13), and POPE/chol (20), M_1 either increases or increases and then saturates with added sterol. This complex behavior has, however, been observed in other membrane properties. Hodzic et al. (23) investigated bilayer thicknesses of POPC/chol and POPC/stigmasterol by x-ray scattering. They found that the bilayer thickness saturates at 20% and decreases as sterol increases from 30 to 40% at 25°C. If the POPE acyl chain length were linearly related to the average chain order parameter in the manner proposed by Seelig and Seelig (28), chain ordering would reflect an increase in bilayer thickness. In this aspect, the results of Hodzic et al. (23) would

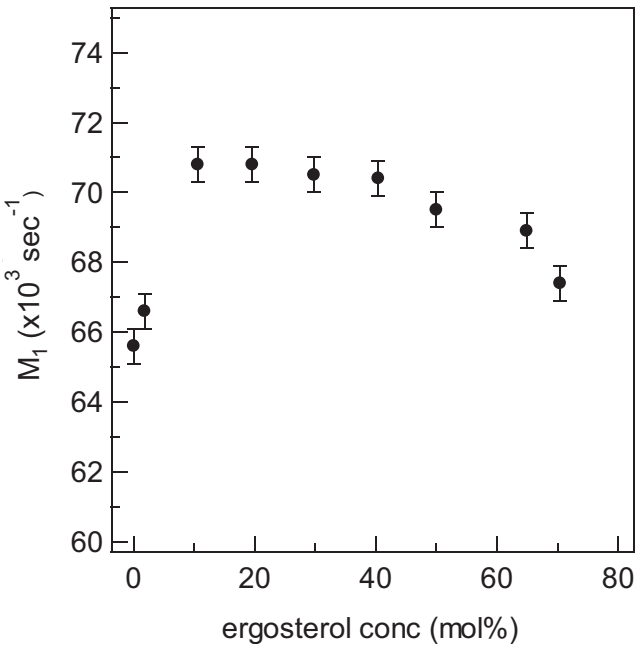

FIGURE 5 M_1 as a function of ergosterol concentration at $T = 25$°C.

be similar to ours for POPE/erg. This interpretation, however, requires further investigation.

To further our understanding of the properties of POPE-d31/erg in the lc phase, we present in Fig. 6 *A* dePaked spectra, which were calculated from the spectra at 25°C. The quadrupolar splitting in the dePaked spectrum is directly proportional to the chain segmental order. The high-frequency peaks, i.e., those with large quadrupolar splittings, correspond to signals from methylene positions near the aqueous interface whereas the resolved low-frequency peaks are associated with the methylene positions and the methyl group in the terminal portion of the chain (29). All the individual peaks and the largest quadrupolar splitting were found to shift to higher frequencies as the ergosterol concentration is increased from 0 to 10 mol %. This result, as well as the data for the smooth order profile (not shown), shows that ergosterol increases the order of the entire POPE acyl chain. The peak positions, however, remain the same as the ergosterol concentration increases from 10 to 40 mol %. As ergosterol concentration is increased to 50 mol %, each peak between 0–30 kHz shifts to lower frequency, resulting in a decrease in quadrupolar splitting that becomes more pronounced at 65 and 70 mol %. These findings indicate that increasing ergosterol concentration from 40 to 70 mol % decreases the order of the terminal portion of the POPE chain.

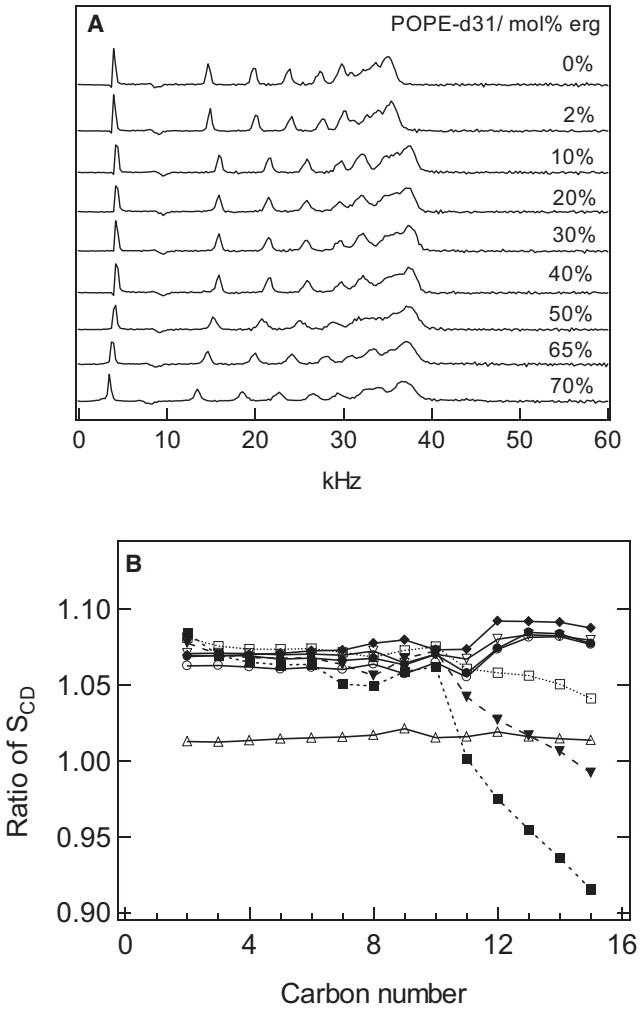

FIGURE 6 (*A*) dePaked spectra of POPE-d31/erg as a function of ergosterol concentration at $T = 25°C$. (*B*) The ratios of order profiles $|S_{CD}|$ using the order profile of pure POPE-d31 as the common denominator at $T = 25°C$ at various ergosterol concentrations. (△) 2 mol %; (◆) 10 mol %; (○) 20 mol %; (▽) 30 mol %; (● 40 mol %; (□) 50 mol %; (▼), 65 mol %; and (■) 70 mol %. All lines are guide to the eyes.

Another way of looking at the effect of ergosterol along the chain is to plot the ratio of the smoothed order profile, $|S_{CD}|$ with the smoothed order profile of pure POPE-d31 as the common denominator. Fig. 6 *B* shows the ratios of the order profiles for POPE-d31 membranes containing 10–40 mol % ergosterol samples have similar shapes, the ratios for C11–15 being larger than those for C2–10. This suggests that the ordering effect is more pronounced at C11–15, the terminal region of the acyl chain, than at C2–10, which are close to the aqueous interface of the membrane. Similar behavior was also found for other lipid/sterol systems such as POPC-d31/chol (30) and DPPC/erg (11). In 50–70 mol % ergosterol samples, the shapes of the ratios of order profiles change dramatically and the major changes occur at C11–15. In particular, the ratios for C11–15 are smaller than those for C2–10. This indicates that the ordering effect is less pronounced at C11–15 than at C2–10. It is of interest to note that increasing ergosterol concentration from 10 to 70 mol % causes the C11–15 portion to change noticeably from a more to a less ordered state at ~40 mol %. This change is most dramatic toward the methyl terminus of the acyl chains. Here C15 of the 65 mol % POPE-d31/erg membrane (with ratio equal 0.99) and C12–15 of the 70 mol % POPE-d31/erg membrane are even more disordered than for pure POPE-d31 (with ratio = 1). The ratios of order profiles at other temperatures, particularly those for 50 and 65 mol % at 19°C, exhibit the same behavior. In addition, the difference order parameter profile obtained by subtracting the smoothed order profile of pure POPE-d31 (not shown), also representing the effect of ergosterol along the chain, shows the same results as in Fig. 6 *B*. Therefore increasing ergosterol concentration from 40 to 70 mol % decreases the order of the terminal portion of the POPE chain, and this is the main contribution leading to the decrease in M_1 above 40 mol % ergosterol in Fig. 5.

We now return to Fig. 4 to discuss the behavior of POPE-d31/erg at high temperature. Above 35°C, the sharp decrease in each $M_1(T)$ curve is associated with the lc to H_{II} phase transition. For example, the $M_1(T)$ curve for 10 mol % ergosterol exhibits an abrupt change beginning at 50°C and ending at 61°C. The spectra describing the phase behavior in this temperature range are shown in Fig. 7. Below 50°C, POPE-d31/erg exhibits a lc spectrum as shown in Fig. 7 *A*. Above 61°C, POPE-d31 shows a spectrum typical of the H_{II} phase as shown in Fig. 7 *D*. The center of the spectrum exhibits an isotropic peak that has ~1% of the total intensity.

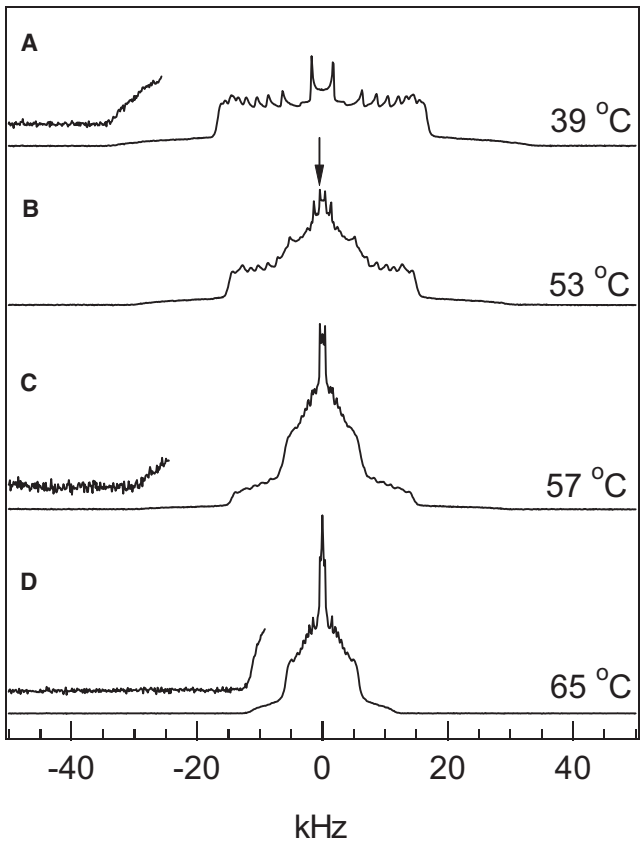

FIGURE 7 ^{2}H NMR spectra of 90:10 POPE-d31/erg.

This could be indicative of a micellar phase, a cubic phase, or another isotropic phase (31,32). The spectrum between 50°C and 61°C, as shown in Fig. 7, *B* or *C*, is a superposition of lc and H_{II} components, indicating a lc + H_{II} phase coexistence. The transition midpoint shown in Fig. 4 shifts from ~65°C for 0 mol % ergosterol to ~43°C for 65 mol % ergosterol, showing that ergosterol markedly decreases the lc to H_{II} transition temperature.

The temperature-composition phase diagram

The phase behavior of POPE-d31/erg discussed above is summarized in the temperature-composition diagram in Fig. 8. The maximum value of M_1 in the lc phase at 25°C (~70,800 s^{-1}, shown in Fig. 5) is markedly less than the M_1 value of the lo phase of POPE/chol (e.g., 84,300 s^{-1} for 70:30 POPE/chol) at the same temperature. This suggests that there is no lo phase behavior for POPE/erg membranes. Two phase coexistence regions are observed: gel + lc phase coexistence at lower temperatures, and lc + H_{II} phase coexistence at higher temperatures.

The lower boundary of the gel + lc region, i.e., the gel/gel + lc boundary, slopes downward from 17°C at 2 mol % toward 3°C at 20 mol %, showing that ergosterol facilitates the formation of the lc phase. The upper boundary of the gel + lc region for samples containing 10–40 mol % ergosterol is relatively flat, whereas for ergosterol concentrations >40 mol %, it decreases with increasing ergosterol from 20°C at 40 mol % to 11°C at 72 mol %. This shows that the temperatures of completion of the main phase transition are close for POPE/erg membranes with concentrations from 10 to 40 mol % and decrease with increasing ergosterol concentrations greater than 40 mol %.

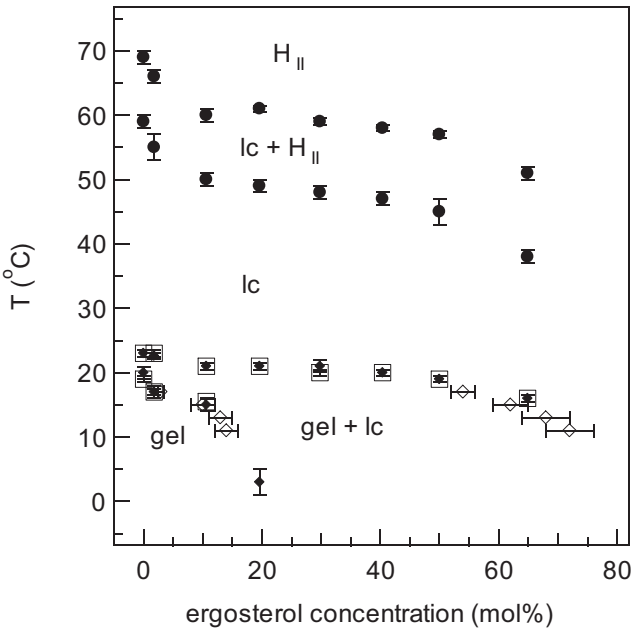

FIGURE 8 Temperature-composition phase diagram of the POPE-d31/erg membrane. (◆) determined by inspection of the spectra as a function of temperature;(□) onset or end of gel-to-lc transition in $M_1(T)$ curves (Fig. 4); (◇) obtained from spectral subtraction as discussed in Fig. 2; and (●) onset or end of lc-to-H_{II} transition in $M_1(T)$ curves (Fig. 4).

The validation of spectral subtraction used for determining the gel + lc phase boundaries (see discussion of Fig. 2) confirms that the proportion of the lc phase increases as ergosterol concentration increases. In addition, as presented in Fig. 4, M_1 decreases progressively with increasing ergosterol concentration. These results show that ergosterol fully incorporates into POPE bilayers up to at least 65 mol % below the main phase transition.

In Fig. 8, the temperatures for the beginning and the end of the lc to H_{II} phase transition (i.e., the lc + H_{II} boundaries) decrease with increasing ergosterol concentration between 0 and 10 mol %. This shows that ergosterol facilitates the formation of the H_{II} phase. Further addition of ergosterol up to 40 mol % does not affect the lc to H_{II} phase transition significantly. Above 40 mol % ergosterol, the transition temperature decreases noticeably again as ergosterol concentration increases to at least 65 mol %.

The liquid-crystalline phase of POPE-d31/erg: discussion and comparison with previous work

We now examine the ergosterol concentration dependence of the lc phase. There has been some discussion in the literature

concerning the saturation of acyl-chain order due to ergosterol in lipid/erg systems. A DPH fluorescence study shows that the acyl-chain order of POPC becomes saturated at ~20 mol % ergosterol (33). The saturation of POPC chain order is also observed at ~25 mol % ergosterol by ^{2}H NMR, and is attributed to the limit of ergosterol solubility (13). Cholesterol is known to have a solubility limit in PC/chol or PE/chol mixtures (34–38). The excess cholesterol is excluded from the bilayer and forms cholesterol monohydrate crystals (34). The saturation of M_1 shown in Figs. 4 and 5 suggests that ergosterol may have a solubility limit as low as ~10 mol % in lc-phase POPE. Moreover, Huang and Feigenson (39) point out that cholesterol requires coverage by the phospholipid headgroup to avoid unfavorable contact with water. This suggests that the saturation concentration for M_1 in POPE/erg is considerably lower than that for POPC/erg because the smaller polar head of POPE provides less coverage than the larger polar head of POPC. Our observation of saturation concentrations for M_1 in POPE/erg (10 mol %) and POPC/erg (25 mol % from Hsueh et al. (13)) agrees qualitatively with their prediction.

However, the following alternative explanation for the ergosterol concentration dependence of the lc phase is more likely. There are two competing consequences of ergosterol incorporation in the POPE lamellar liquid crystalline phase: chain ordering and bilayer destabilization heralding the onset of the inverted hexagonal phase at higher temperature. At low ergosterol concentrations chain ordering dominates whereas at high concentrations bilayer destabilization dominates. At intermediate concentrations, the two effects compete with one another resulting in the observed M_1 plateau. Thus there is no need to invoke the formation of ergosterol monohydrate for POPE/erg membranes.

Comparison of the properties of POPE/erg and POPE/chol membranes

It is useful at this point to compare the experimental results for POPE/erg with those of POPE/chol. Fig. 9 shows M_1 for 80:20 and 70:30 POPE-d31/chol. This figure shows that M_1 decreases with increasing cholesterol below 17°C. Furthermore, both ergosterol and cholesterol disrupt the gel phase of POPE membranes though the reduction in M_1 caused by ergosterol is smaller than that caused by cholesterol. For example, M_1 decreases by only 2% with addition of 20 mol % ergosterol at 11°C, whereas it decreases by 12% with the same amount of cholesterol at this temperature. Ergosterol is therefore less effective than cholesterol in disordering gel-phase POPE. Above 22°C, M_1 increases with increasing cholesterol concentration. In contrast, M_1 for POPE/erg saturates at 10 mol % ergosterol. Thus ergosterol is far less effective than cholesterol in ordering lc phase POPE.

We next compare the temperature-composition phase diagrams of POPE-d31/erg of Fig. 8 with that of POPE/chol for sterol concentrations between 0 to 45 mol % (20). At temperatures below the completion of the respective gel/liquid phase transition, both diagrams exhibit the coexistence of the gel phase with a liquid phase, which is the lc phase for POPE/erg and the lo phase for POPE/chol. Although the lc phase of POPE/erg and the lo phase of POPE/chol are both rich in sterol, the lc phase exhibits an acyl chain order that is considerably smaller than that of the lo phase. The (gel + lc)/lc boundary, characterizing the composition of the lc phase within the two-phase region of POPE/erg, slopes much further toward higher ergosterol concentrations than the L_β(or gel)+lo/lo boundary of POPE/chol. For example, in the gel + lc region, the composition of the lc phase of POPE/erg is ~62 mol % ergosterol at 15°C, which is three times larger than that of the lo phase of POPE/chol. This shows that more ergosterol than cholesterol is required for the formation of the relevant liquid phase. Thus, ergosterol is far less effective than cholesterol in inducing a liquid phase in gel-phase POPE membranes.

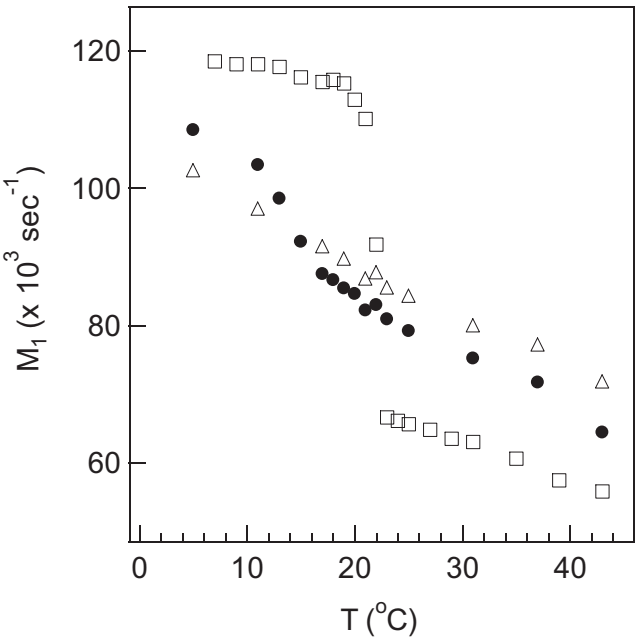

FIGURE 9 Temperature dependence of M_1 for POPE-d31/chol at various cholesterol concentrations. (□), 0 mol %; (●), 20 mol %; and (△) 30 mol %. The $M_1(T)$ for pure POPE-d31 is presented again as a reference.

Both temperature-composition phase diagrams show the coexistence of lc and H_{II} phases at high temperatures. The lower boundaries of the coexistence regions of both systems are more or less similar below 40 mol %. Furthermore, the values of the lc/H_{II} phase transition temperature, T_h, of both systems decreases as sterol increases up to 10 mol %, suggesting that both sterols facilitate the formation of the H_{II} phase. T_h is less sensitive to ergosterol concentration than cholesterol concentration between 10 and 40 mol %. In addition, T_h of POPE/chol increases as the cholesterol concentration increases from 40 to 45 mol %, whereas that

of POPE/erg decreases as the ergosterol concentration increases from 40 to 65 mol %. At concentrations above 40 mol %, cholesterol tends to stabilize POPE bilayers, whereas ergosterol tends to destabilize them. Because ergosterol causes the acyl chain order of the terminal portion of the POPE chain to decrease in the lc phase as shown in Fig. 6, an enhanced cone shape for the POPE molecule would be expected. This destabilizes the POPE bilayer structure and causes T_h of POPE/erg to decrease. In the case of POPE/chol, Paré and Lafleur (20) argue that the acyl chain ordering effect by cholesterol dominates at high cholesterol concentrations, which stabilizes POPE bilayers and increases T_h.

CONCLUSIONS

We have shown that addition of ergosterol disrupts the gel-phase POPE membrane, forming a lc phase whose proportion increases with ergosterol content until the gel phase is abolished at high (>50 mol %) sterol concentrations. Above T_m, ergosterol has a complex effect on lc-phase POPE. At low concentrations (up to 10 mol %) adding ergosterol increases POPE chain order, however adding more ergosterol (from 10 to 40 mol %) causes no further ordering. The capacity of ergosterol to disorder the POPE gel phase thus contrasts dramatically with its very limited ability to order the lc phase of POPE membranes. This difference has not as yet been observed in POPE/chol or other PC/sterol systems.

Increasing the ergosterol content of the membrane from 40 to 70 mol % causes the C11–16 section of POPE's palmitoyl chain to become markedly less ordered, consistent with an enhanced cone shape for POPE within the lc bilayers. This phenomenon is unusual and, to our knowledge, our data represents the first observation of this type in lipid/sterol systems. It would be interesting to extend this observation to other lipid/sterol systems with higher concentrations of sterol (>40 mol %). More studies are in progress.

Ergosterol and cholesterol have similar disrupting effects on gel-phase POPE, but the former does not disorder POPE as effectively as the latter. Moreover, ergosterol has markedly different effects on the lc phase of POPE membranes as compared with cholesterol: cholesterol progressively increases the average chain order of POPE-d31 up to a concentration of at least 45 mol % (20). However, ergosterol and cholesterol share a common molecular structure with small modifications: ergosterol has an extra double bond at C7–C8 in its fused rings and, on its flexible tail, an extra double bond at C22–C23 plus an extra methyl group at C24. These small modifications in sterol structure are important determinants of POPE-sterol interactions, and can result in distinct differences in lipid membrane properties, particularly in the lc phase.

The temperature-composition phase diagram of POPE-d31/erg was determined from the ^{2}H NMR spectra. It exhibits a gel and ergosterol-rich lc phase coexistence (gel + lc) region at low temperatures, and an lc + H_{II} phase coexistence at high temperatures. The saturation of POPE acyl chain order at 10 mol % ergosterol is a property of the lc phase of POPE/erg. In the ergosterol-rich part of the lc phase (ergosterol >40 mol %), POPE chain order decreases with increasing ergosterol. Note that at all ergosterol concentrations, the lc-phase POPE's acyl chain order is much smaller than that of comparable POPE/chol membranes. This implies that there is no lo phase behavior for POPE/erg membranes.

We propose two possible explanations for the unusual effect of ergosterol on lc-phase POPE membranes. First, ergosterol may be exerting two competing influences on lc-phase POPE, chain-ordering, and hexagonal-phase stabilization. At low ergosterol concentrations, the chain ordering effect dominates, whereas at concentrations >40 mol % ergosterol fluctuations that predispose the membrane to adopt the inverted hexagonal phase have a larger effect. The dramatic reduction in the bilayer to hexagonal transition temperature with increasing ergosterol content is strong evidence for this interpretation. Second, ergosterol could have a solubility limit as low as ~10 mol % in lc-phase POPE causing M_1 to saturate. As the nominal ergosterol concentration increases to above 40 mol %, ergosterol crystallites may then interfere with POPE lipid packing in such a way that the POPE acyl chain order in the lc phase decreases. We have observed recently that the DPPC/erg M_1 decreases from 50 to 80 mol % ergosterol (Y.-W. Hsueh, unpublished) that is quite likely a manifestation of the same solubility behavior. No such limit to ergosterol solubility in gel phase POPE was observed. This explains why the ability of ergosterol to disorder the gel-phase of POPE membranes is so much larger than its ability to order their lc phase. Furthermore, the apparent low solubility of ergosterol in the lc phase-POPE membrane may have consequences regarding the distribution of ergosterol in yeast PMs. Yeast PMs are composed of ergosterol, sphingolipids, and phosphoglycerolipids mostly with one chain unsaturated. Assuming that ergosterol has limited solubility in these unsaturated phospholipids and that yeast PM rafts are largely composed of ergosterol and yeast sphingolipids, the ergosterol concentration of these rafts as a result would be enriched to a greater extent than, for example, analogous rafts containing cholesterol in place of ergosterol.

This work was supported by the National Science Council of Taiwan (NSC 92-2112-M-008-049, NSC 93-2112-M-008-003) and the Natural Sciences and Engineering Research Council of Canada.

REFERENCES

1. Gennis, R. B. 1989. Biomembranes, Molecular Structure and Function. Springer-Verlag, New York.
2. Longley, R. P., A. H. Rose, and B. A. Knights. 1968. Composition of the protoplast membrane from *Saccharomyces cerevisiae*. *Biochem. J.* 108:401–412.
3. Tuller, G., T. Nemec, …, G. Daum. 1999. Lipid composition of subcellular membranes of an FY1679-derived haploid yeast wild-type strain grown on different carbon sources. *Yeast*. 15:1555–1564.

4. Bagnat, M., S. Keränen, …, K. Simons. 2000. Lipid rafts function in biosynthetic delivery of proteins to the cell surface in yeast. *Proc. Natl. Acad. Sci. USA*. 97:3254–3259.
5. Bagnat, M., A. Chang, and K. Simons. 2001. Plasma membrane proton ATPase Pma1p requires raft association for surface delivery in yeast. *Mol. Biol. Cell*. 12:4129–4138.
6. Malinska, K., J. Malinsky, …, W. Tanner. 2004. Distribution of Can1p into stable domains reflects lateral protein segregation within the plasma membrane of living *S. cerevisiae* cells. *J. Cell Sci*. 117: 6031–6041.
7. Zabrocki, P., I. Bastiaens, …, J. Winderickx. 2008. Phosphorylation, lipid raft interaction and traffic of α-synuclein in a yeast model for Parkinson. *Biochim. Biophys. Acta*. 1783:1767–1780.
8. Vist, M. R., and J. H. Davis. 1990. Phase equilibria of cholesterol/dipalmitoylphosphatidylcholine mixtures: ^{2}H nuclear magnetic resonance and differential scanning calorimetry. *Biochemistry*. 29:451–464.
9. Almeida, P. F. F., W. L. C. Vaz, and T. E. Thompson. 1992. Lateral diffusion in the liquid phases of dimyristoylphosphatidylcholine/cholesterol lipid bilayers: a free volume analysis. *Biochemistry*. 31: 6739–6747.
10. Thewalt, J. L., and M. Bloom. 1992. Phosphatidylcholine: cholesterol phase diagrams. *Biophys. J*. 63:1176–1181.
11. Hsueh, Y.-W., K. Gilbert, …, J. Thewalt. 2005. The effect of ergosterol on dipalmitoylphosphatidylcholine bilayers: a deuterium NMR and calorimetric study. *Biophys. J*. 88:1799–1808.
12. Wu, R., L. Chen, …, P. J. Quinn. 2006. Phase diagram of stigmasterol-dipalmitoylphosphatidylcholine mixtures dispersed in excess water. *Biochim. Biophys. Acta*. 1758:764–771.
13. Hsueh, Y.-W., M.-T. Chen, …, J. Thewalt. 2007. Ergosterol in POPC membranes: physical properties and comparison with structurally similar sterols. *Biophys. J*. 92:1606–1615.
14. Miao, L., M. Nielsen, …, O. G. Mouritsen. 2002. From lanosterol to cholesterol: structural evolution and differential effects on lipid bilayers. *Biophys. J*. 82:1429–1444.
15. Urbina, J. A., S. Pekerar, …, E. Oldfield. 1995. Molecular order and dynamics of phosphatidylcholine bilayer membranes in the presence of cholesterol, ergosterol and lanosterol: a comparative study using ^{2}H-, ^{13}C- and ^{31}P-NMR spectroscopy. *Biochim. Biophys. Acta*. 1238: 163–176.
16. Endress, E., H. Heller, …, T. M. Bayerl. 2002. Anisotropic motion and molecular dynamics of cholesterol, lanosterol, and ergosterol in lecithin bilayers studied by quasi-elastic neutron scattering. *Biochemistry*. 41:13078–13086.
17. Endress, E., S. Bayerl, …, T. M. Bayerl. 2002. The effect of cholesterol, lanosterol, and ergosterol on lecithin bilayer mechanical properties at molecular and microscopic dimensions: a solid-state NMR and micropipet study. *Langmuir*. 18:3293–3299.
18. Shahedi, V., G. Orädd, and G. Lindblom. 2006. Domain-formation in DOPC/SM bilayers studied by pfg-NMR: effect of sterol structure. *Biophys. J*. 91:2501–2507.
19. Paltauf, F., S. D. Kohlwein, and S. A. Henry. 1992. Regulation and compartmentalization of lipid synthesis in yeast. *In* The Molecular and Cellular Biology of the Yeast *Saccharomyces*: Gene Expression. E. W. Jones, J. R. Pringle, and J. R. Broach, editors. Cold Spring Harbor Laboratory, Cold Spring Harbor, NY. 415–500.
20. Paré, C., and M. Lafleur. 1998. Polymorphism of POPE/cholesterol system: a ^{2}H nuclear magnetic resonance and infrared spectroscopic investigation. *Biophys. J*. 74:899–909.
21. Blume, A., and R. G. Griffin. 1982. Carbon-13 and deuterium nuclear magnetic resonance study of the interaction of cholesterol with phosphatidylethanolamine. *Biochemistry*. 21:6230–6242.
22. Brown, M. F., and J. Seelig. 1978. Influence of cholesterol on the polar region of phosphatidylcholine and phosphatidylethanolamine bilayers. *Biochemistry*. 17:381–384.
23. Hodzic, A., M. Rappolt, …, G. Pabst. 2008. Differential modulation of membrane structure and fluctuations by plant sterols and cholesterol. *Biophys. J*. 94:3935–3944.
24. Davis, J. H., K. R. Jeffrey, …, T. P. Higgs. 1976. Quadrupolar echo deuteron magnetic resonance spectroscopy in ordered hydrocarbon chains. *Chem. Phys. Lett*. 42:390–394.
25. Lafleur, M., B. Fine, …, M. Bloom. 1989. Smoothed orientational order profile of lipid bilayers by ^{2}H-nuclear magnetic resonance. *Biophys. J*. 56:1037–1041.
26. Hsueh, Y.-W., M. Zuckermann, and J. Thewalt. 2005. Phase diagram determination for phospholipids/sterol membranes using deuterium NMR. *Concepts in Magn. Reson. Part A*. 26A:35–46.
27. Davis, J. H., and K. R. Jeffrey. 1977. The temperature dependence of chain order in potassium palmitate-water. A deuterium NMR study. *Chem. Phys. Lipids*. 20:87–104.
28. Seelig, A., and J. Seelig. 1977. Effect of a single cis double bond on the structures of a phospholipid bilayer. *Biochemistry*. 16:45–50.
29. Lafleur, M., P. R. Cullis, …, M. Bloom. 1990. Comparison of the orientational order of lipid chains in the L_α and H_{II} phases. *Biochemistry*. 29:8325–8333.
30. Lafleur, M., P. R. Cullis, and M. Bloom. 1990. Modulation of the orientational order profile of the lipid acyl chain in the L_α phase. *Eur. Biophys. J*. 19:55–62.
31. Shyamsunder, E., S. M. Gruner, …, C. P. Tilcock. 1988. Observation of inverted cubic phase in hydrated dioleoylphosphatidylethanolamine membranes. *Biochemistry*. 27:2332–2336.
32. El Jastimi, R., and M. Lafleur. 1999. Nisin promotes the formation of non-lamellar inverted phases in unsaturated phosphatidylethanolamines. *Biochim. Biophys. Acta*. 1418:97–105.
33. Arora, A., H. Raghuraman, and A. Chattopadhyay. 2004. Influence of cholesterol and ergosterol on membrane dynamics: a fluorescence approach. *Biochem. Biophys. Res. Commun*. 318:920–926.
34. Guo, W., and J. A. Hamilton. 1995. A multinuclear solid-state NMR study of phospholipid-cholesterol interactions. Dipalmitoylphosphatidylcholine-cholesterol binary system. *Biochemistry*. 34:14174–14184.
35. Huang, J., J. T. Buboltz, and G. W. Feigenson. 1999. Maximum solubility of cholesterol in phosphatidylcholine and phosphatidylethanolamine bilayers. *Biochim. Biophys. Acta*. 1417:89–100.
36. Brzustowicz, M. R., V. Cherezov, …, S. R. Wassall. 2002. Molecular organization of cholesterol in polyunsaturated membranes: microdomain formation. *Biophys. J*. 82:285–298.
37. Shaikh, S. R., V. Cherezov, …, S. R. Wassall. 2003. Interaction of cholesterol with a docosahexaenoic acid-containing phosphatidylethanolamine: trigger for microdomain/raft formation? *Biochemistry*. 42:12028–12037.
38. Shaikh, S. R., V. Cherezov, …, S. R. Wassall. 2006. Molecular organization of cholesterol in unsaturated phosphatidylethanolamines: x-ray diffraction and solid state ^{2}H NMR reveal differences with phosphatidylcholines. *J. Am. Chem. Soc*. 128:5375–5383.
39. Huang, J., and G. W. Feigenson. 1999. A microscopic interaction model of maximum solubility of cholesterol in lipid bilayers. *Biophys. J*. 76:2142–2157.